Thermal Infrared Imaging: A Novel Method to Monitor Airflow During Polysomnography

Jayasimha N. Murthy, MD, D.ABSM[1]; Johan van Jaarsveld, MD[1]; Jin Fei, PhD[2]; Ioannis Pavlidis, PhD[2]; Rajesh I Harrykissoon, MD[1]; Joseph F. Lucke, PhD[3]; Saadia Faiz, MD[1]; Richard J. Castriotta, MD, D.ABSM[1]

[1]Division of Pulmonary, Critical Care and Sleep Medicine, University of Texas Health Science Center at Houston, Houston, TX; [2]Department of Computer Science, University of Houston, Houston, TX; [3]Center for Clinical Research and Evidence Based Medicine, University of Texas Health Science Center at Houston, Houston, TX

Study Objectives: This is a feasibility study designed to evaluate the accuracy of thermal infrared imaging (TIRI) as a noncontact method to monitor airflow during polysomnography and to ascertain the chance-corrected agreement (κ) between TIRI and conventional airflow channels (nasal pressure [Pn], oronasal thermistor and expired CO_2 [P_ECO_2]) in the detection of apnea and hypopnea.
Design: Subjects were recruited to undergo polysomnography for 1 to 2 hours, during which simultaneous recordings from electroencephalography, electrooculography, electromyography, respiratory impedance plethysmography, conventional airflow channels, and TIRI were obtained.
Setting: University-affiliated, American Academy of Sleep Medicine-accredited sleep disorders center.
Patients or Participants: Fourteen volunteers without a history of sleep disordered breathing and 13 patients with a history of obstructive sleep apnea were recruited.
Measurements and Results: In the detection of apnea and hypopnea, excellent agreement was noted between TIRI and thermistor ($\kappa = 0.92$, Bayesian Credible Interval [BCI] 0.86, 0.96; pκ = 0.99). Good agreement was noted between TIRI and Pn ($\kappa = 0.83$, BCI 0.70, 0.90; pκ = 0.98) and between TIRI and P_ECO_2 ($\kappa = 0.80$, BCI 0.66, 0.89; pκ = 0.94).
Conclusions: TIRI is a feasible noncontact technology to monitor airflow during polysomnography. In its current methodologic incarnation, it demonstrates a high degree of chance-corrected agreement with the oronasal thermistor in the detection of apnea and hypopneas but demonstrates a lesser degree of chance-corrected agreement with Pn. Further overnight validation studies must be performed to evaluate its potential in clinical sleep medicine.
Keywords: Sleep apnea syndromes, sleep disordered breathing, sleep apnea, sleep hypopnea, thermography, polysomnography, sleep monitoring
Citation: Murthy JN; van Jaarsveld J; Pavlidis I; Harrykissoon R; Lucke JF; Faiz S; Castriotta RJ. Thermal infrared imaging: a novel method to monitor airflow during polysomnography. *SLEEP* 2009;32(11):1521-1527.

THE DIAGNOSIS OF SLEEP APNEA TYPICALLY IN-VOLVES AN OVERNIGHT POLYSOMNOGRAM WITH CONTINUOUS MONITORING OF SEVERAL PHYSI-OLOGIC parameters and surrogate measures of airflow (nasal pressure [Pn], oronasal thermistor, expired CO_2 waveform [P_ECO_2]) using contact sensors.[1-5] A subject can come in contact with at least 20 such sensors during a study. These sensors and the wires can influence not only the usual sleep architecture, but also the posture of the patient during the study night.[6-8] Contact sensors like nasal prongs and oronasal thermistors are routinely used as surrogate measures of airflow because they are less obtrusive than the reference-standard airflow sensor, namely, the pneumotachometer.[1,9,10] However, the presence of the surrogate airflow sensors and the associated wires in the proximity of the subject's oronasal area can still cause discomfort to the patient during sleep. Contact sensors also have the potential to misalign during the study, requiring repositioning at the bedside by a technician, to obtain good-quality data.

We have demonstrated that measurement of breathing rates is feasible at a distance using thermal infrared imaging (TIRI).[11] The method is based on second-order statistics of the presence or absence of the hot expiratory plume in the vicinity of the nostrils. We have also studied a more advanced method that is based on wavelet analysis of the thermal imaging signal on the nostrils themselves.[12,13] When analyzing the thermal imaging signal, we extracted the full breathing waveform (rate and amplitude). Consistent segmentation of the nostril area and facial tissue-tracking algorithms[14] enabled sustained monitoring of breathing, resulting in functionality equivalent to that of a thermistor, delivered in a contact-free manner. In 5-minute recordings of 20 awake healthy individuals, agreement between breathing waveforms from the virtual (imaging) and contact thermistors was found to be greater than 90%.

The hardware and software system that was developed to implement the latest method is called automatic thermal monitoring system (ATHEMOS). The centerpiece of the system is a midwave infrared camera (FLIR® SC-6000), supported by a black body for calibration and a pan-tilt mechanism for positioning. The system is controlled and the acquired imaging signals are processed by real-time custom software developed in our labs.

ATHEMOS and the imaging method that we reported on in a previous publication[12] constitute the TIRI portion of the present study. The objective in this current study was to determine the efficacy of TIRI to detect apnea and hypopnea by using conventional surrogate airflow sensors as comparison standards during polysomnography. Thus, our hypothesis was that there would be a very high degree of chance-corrected agreement ($\kappa \geq 0.6$) between TIRI and each of the conventional flow
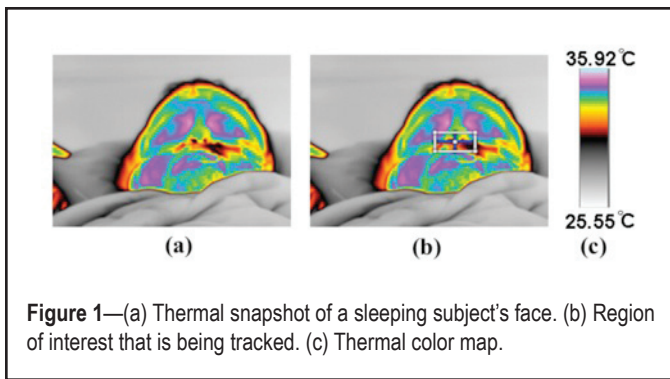
Figure 1—(a) Thermal snapshot of a sleeping subject's face. (b) Region of interest that is being tracked. (c) Thermal color map.

Figure 2—Delineation of the measurement region by segmentation algorithm of the thermal infrared imaging (TIRI). The measurement region fits the nostril area only; this is a subset of the tracking region (see Figure 1), which is broader.

sensors, such as thermistor, Pn, and P_ECO_2 in the detection of apnea and hypopnea. Some of the data from this manuscript has been presented at scientific meetings and published in the form of abstracts.[15,16]

METHODS

Recruitment Procedures

The Institutional Review Board approved the study protocol, and informed consents were obtained from all participants. The study was conducted at the University of Texas Health Science Center at Houston and The Memorial Hermann Hospital Sleep Disorders Center, Houston, Texas. Since this is the first reported study that uses TIRI for airflow monitoring during polysomnography, formal sample-size calculation was not possible. A nonrandom convenience sample of 14 adult volunteers (age 18 years or older**)** from the community, who did not have a diagnosis of sleep disordered breathing, were recruited to participate in the study. Similarly, 13 adult patients who had a prior diagnosis of obstructive sleep apnea by polysomnography were also invited to participate in this study.

Polysomnography and Related Procedures

All subjects underwent polysomnography between 18:00 and 22:00 on the designated day. Central and occipital electroencephalography, electrooculography, chin electromyography, acoustic monitoring of snoring with a microphone, digital pulse oximetry (SpO_2), and conventional airflow monitoring with Pn, oronasal thermistor, and P_ECO_2 were performed. Respiratory effort was recorded using thoracic and abdominal piezoelectric bands and respiratory inductance plethysmography. All recording channels were calibrated according to the standard protocol followed in the sleep disorders center, following which the subjects were instructed to go to sleep. We attempted to obtain at least 60 minutes of recording during sleep for each subject.

ATHEMOS recorded thermal imagery at a mean rate of 30 frames per second. However, due to the load imposed on the operating system from the massive data recording, the recording speed varied by a few frames on either side of the mean. To facilitate harmonic analysis (with the assumption of constant sampling) and ease the computational load, we down-sampled to a constant rate of 10 frames per second. The spatial resolution of each frame was 320 × 256 pixels. The sensitivity of the thermal acquisition was 0.025°C. A tracking algorithm compensated for facial motion within bounds (see Figure 1). An automatic segmentation algorithm (virtual probe) delineated the nostril region and computed the local mean thermal signal, which was the carrier of the breathing information (see Figure 2). The segmenter was cued by the tracker throughout the process.[12] The airflow component of the thermal signal was extracted through wavelet analysis. The 3 major algorithmic components of the thermal imaging methodology are tracking, segmentation, and wavelets analysis.
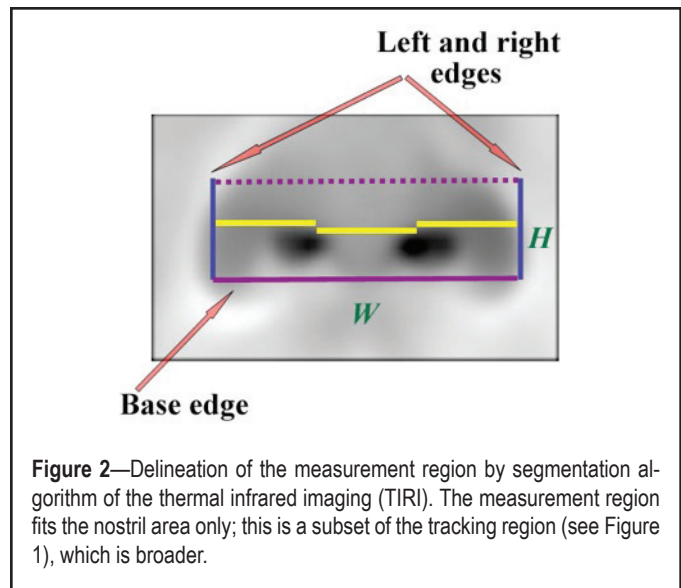
Tracking Facial Tissue in TIRI

Because the face of the subject may move at any point, a tracking algorithm is paramount to the measurement's accuracy. Even small movements that span only a few pixels in the image plane can introduce a substantial error if they are not compensated. In structural imaging (e.g., visual imaging), when the conditions are controlled, the tracking object can be modeled because it is expected to either remain static or change in predictable ways. However, thermal imaging is functional and not structural in nature. It maps thermophysiologic function that is randomly changing and, thus, is difficult to model. The best way to robustly deal with the dynamics of thermal facial imaging is to use trackers based on advanced statistics (particle filter trackers[17]). In fact, one may gain in terms of accuracy and robustness if a network of collaborative particle filter trackers is used instead of a loner. This scheme is known as coalitional tracking, and we were the first to present its design and advantages.[14]

Nostril Segmentation in TIRI

Due to expiration and inspiration, there is temporal variation in the thermal signature of the nostrils. If the nostrils were accurately localized in thermal imagery, then computing their mean temperature over time would act as a remote nasal thermistor. In thermal imagery, the nostrils can be segmented from the rest of the facial tissue due to colder boundaries formed by cartilage. Segmentation is achieved by performing integral projections on the edge image of the face. The edge image is produced by applying the Sobel edge detector on the original thermal image.[18]

Breathing Waveform Through Wavelet Analysis

The thermal signal produced from the mean temperature of the segmented nostril region over time carries the breathing in-
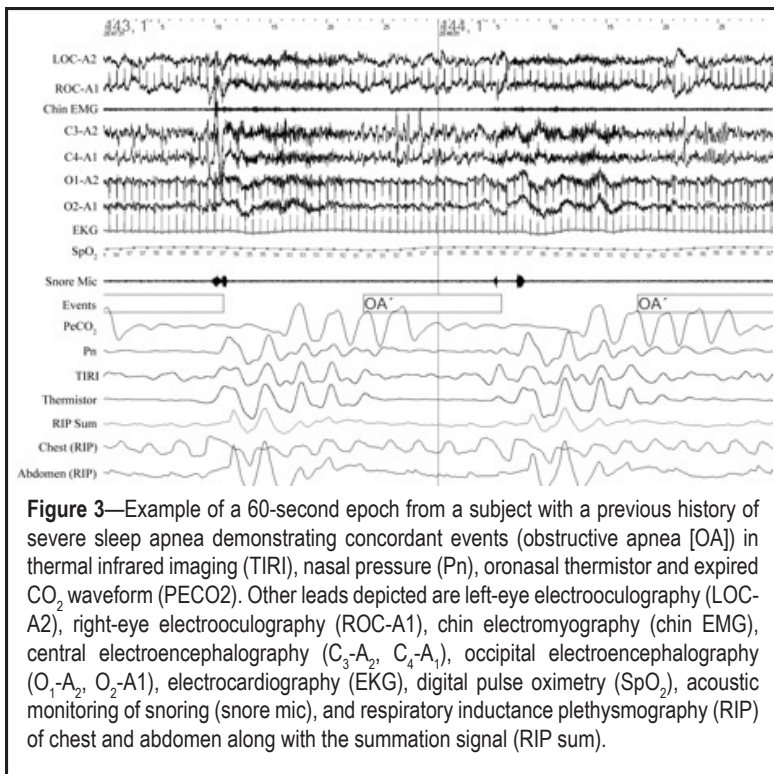
Figure 3—Example of a 60-second epoch from a subject with a previous history of severe sleep apnea demonstrating concordant events (obstructive apnea [OA]) in thermal infrared imaging (TIRI), nasal pressure (Pn), oronasal thermistor and expired CO_2 waveform (PECO2). Other leads depicted are left-eye electrooculography (LOC-A2), right-eye electrooculography (ROC-A1), chin electromyography (chin EMG), central electroencephalography (C_3-A_2, C_4-A_1), occipital electroencephalography (O_1-A_2, O_2-A1), electrocardiography (EKG), digital pulse oximetry (SpO_2), acoustic monitoring of snoring (snore mic), and respiratory inductance plethysmography (RIP) of chest and abdomen along with the summation signal (RIP sum).

formation. In fact, the assumption is that the breathing component is the strongest part of the thermal signal. To isolate the pure breathing waveform from other components (e.g., noise), wavelet analysis is performed. Specifically, continuous wavelet transformation (CWT) is performed on the normalized thermal signal $S'(t)$:

$$\psi_{S'}^{\psi}(\tau,s) = \frac{1}{\sqrt{s}} \int S'(t) \Psi\left(\frac{t-\tau}{s}\right) dt, \qquad (1)$$

where Ψ is the mother wavelet (Mexican hat in this case), τ represents the translation parameter, while s denotes the scale at which the signal is examined. The signal needs to be examined at $s = s_{max}$ corresponding to a local maximum of the wavelet energy coefficients, where the breathing component is expected to reside:

$$s_{max} = \arg \max_i \left\{ \sum |WT_i|(t)^2 \right\}, \qquad (2)$$

Integration of ATHEMOS with Polysomnography

The thermal signal acquired by the camera and processed by ATHEMOS was not only recorded into digital media, but also integrated into the existing polysomnography system (Embla®/Rembrandt®) as an airflow channel by a digital-to-analog converter. This allowed for easy display and comparison of all the airflow channels on a single monitor. An additional nasal thermistor and thoracoabdominal piezoelectric bands were used as controls for the digital-to-analog converter, with their signal being sent directly into the ATHEMOS computer. System clocks on both the ATHEMOS computer and the polysomnographic system were synchronized manually prior to each study

so that events recorded on both systems could be referenced based on time stamps.

Scoring of Sleep Studies

All studies were scored in 30-second epochs. Sleep staging was done according to Rechtschaffen and Kales criteria,[19] and respiratory events were scored as previously described.[20] Apnea was defined as at least a 90% decrease in flow-sensor signal. A hypopnea was defined as a decrease in airflow signal by at least 50% from the baseline with a 4% or greater oxygen desaturation from preevent baseline. All studies were scored by 1 of the investigators. During scoring, a single airflow channel was displayed and examined for events. The scorer was blinded to the events in the other airflow channels. Following this, events and nonevents could not be rescored. The number of apneas and hypopneas and the apnea-hypopnea index were computed for each of these airflow channels. The entire study was reanalyzed by visualizing TIRI with a reference airflow channel (Pn and thermistor) for concordant and discordant events. We defined, a priori, a concordant event (apnea or hypopnea) to have at least a 50% overlap (duration) with the same event recorded in the comparison channel. A discordant event was defined as having a less than 50% overlap. Any epoch with an event, or a continuation of an event from a previous epoch, was called an *event epoch*. All others were *nonevent epochs*. A concordant event epoch had to demonstrate concordance between TIRI and a reference channel for all events. An additional allowance between 5 and 10 seconds of expected delay was taken into consideration while determining the concordance of events recorded in the P_ECO_2 channel in comparison with either TIRI or other reference channels. An example of events demonstrating concordance across all airflow channels (TIRI, Pn, thermistor, and P_ECO_2) is depicted in Figure 3.

Statistical Analysis

Methods

Descriptive statistics were used to summarize the baseline characteristics of the study subjects.

Statistical Model for κ Estimation

The data analyzed consisted of a large number (119-181) of epochs from relatively few patients (14 controls and 13 patients with obstructive sleep apnea [OSA]). A Bayesian, longitudinal, random-effects, Bernoulli model was utilized, accounting for the probability of the occurrence of events (device effect) in each of the airflow channels, (TIRI, Pn, oronasal thermistor, or P_ECO_2) and their corresponding joint probability, as well as each subject's influence on these probabilities.

The subject effect was assumed to be random, following a normal distribution, and the device effects and agreement effects were assumed to be fixed. To complete the Bayesian specification, vague or weakly informative prior distributions were adopted for the parameters. Markov chain Monte Carlo methods were used to obtain the posterior distributions and were conducted in OpenBUGS 3.0.3; additional analyses were con-

Table 1—Baseline Characteristics of Subjects Who Underwent Polysomnography

Parameter	Subjects	
	OSA	No OSA
No.		
Women	5	6
Men	9	7
Age, y	38.9 ± 11 (24-61)	49.8 ± 14 (27-68)
Height, in.	67.5 ± 2.9 (63-72)	66.80 ± 4.9 (60-75)
Weight, lbs.	180.7 ± 41.5 (130-175)	228.5 ± 62.7 (130-344)
BMI, kg/m2	27.8 ± 5.9 (19.7-40.5)	35.5 ± 7.1 (23-45.6)
Neck circumference, cm	40.5 ± 3.5 (31.5-46)	40.1 ± 9 (21-54)
Blood pressure, mm Hg		
Systolic	121 ± 13.6 (94-142)	122 ± 12.8 (106-156)
Diastolic	71 ± 7.4 (60-84)	76 ± 9.2 (60-90)
Mallampatti score	2 (1-3)	3 (1-4)
ESS Score	8 ± 5 (1-19)	12 ± 5.5 (1-19)
AHI on prior sleep study	NA	44.4 ± 31.3 (10.7-110)

Data are presented as mean ± SD (range), except sex, which is reported as a number, and Mallampatti score, which is reported as a median. OSA, obstructive sleep apnea; BMI, body mass index; ESS, Epworth Sleepiness Scale; AHI, apnea-hypopnea index.

Table 2—Number of Event Epochs "Missed" by Each Flow Channel When an Event Epoch was Scored Using the 3 other Comparison Channels

Channel in question[a]	Epoch events	
	Total[b]	Missed[c]
Nasal pressure	165	1 (0.6)
TIRI	167	3 (1.8)
Thermistor	185	21 (11.35)
P_ECO_2	193	29 (15.02)

[a]The comparison channels included all 3 channels other than the channel in question.
[b]Total number of event epochs identified in the 3 reference channels.
[c]Number (%) of event epochs "missed" by the channel in question.
TIRI, thermal infrared imaging; P_ECO_2, expired carbon dioxide.

ducted in R 2.6.2 and STATA 10. A more detailed description of the statistical method is included in the online appendix.

RESULTS

Demographic Data

The demographic characteristics of subjects with and without a previous diagnosis of OSA have been delineated in Table 1. One subject who did not have a history of sleep disordered breathing had a significant number of apneas and hypopneas during this study and was subsequently referred for a full nocturnal polysomnogram. However, for the purposes of our analysis, the data collected from that subject were analyzed along with the subjects who did not have a history of OSA. The group of subjects with a diagnosis of OSA was heavier (mean body mass index = 35.5 ± 7.1 kg/m² [SD] vs 27.8 ± 5.9 kg/m², P = 0.005) and older (mean age 49.8 ± 14 years vs 38.9 ± 11 years, P = 0.03). There were no other significant differences between the 2 groups in physical findings or sleep architecture. The mean total recording time was 109.5 ± 23.9 minutes in the non-OSA group, and 105.9 ± 13 minutes in the OSA group. Overall, there was decreased sleep efficiency (53 ± 25.3 % in non-OSA; 52.7 ± 23.8 % in OSA group) and increased sleep latency (18.6 ± 22.21 minutes in non-OSA; 18.6 ± 13 minutes in OSA group) in both groups. Sleep architecture was dominated by non-rapid eye movement stage 2 sleep in both groups. Subjects with a prior diagnosis of OSA had a baseline mean apnea-hypopnea index of 44.4 ± 31.3 (range 10.7-110).

Agreement Between TIRI and Each of the Reference Channel

There were 167 concordant event epochs detected by all 3 conventional flow channels, with 3 event epochs (1.8%) "missed" by TIRI (see Table 2). There were 2 "false positive"

event epochs identified by TIRI when 4170 epochs were determined to be event free by Pn, thermistor, and P_ECO_2 concordance. There was a high degree of agreement between TIRI, Pn, thermistor, and P_ECO_2 when any combination of 2 comparison channels was considered. The distributions of concordant and discordant events between TIRI and the conventional channels are outlined in Table 3. There was 99.6% agreement between Pn and TIRI, with κ = 0.83 (see Table 4). Likewise, the agreement between TIRI and thermistor (99.2% agreement, κ = 0.92, Bayesian Credible Interval [BCI] 0.86, 0.96; pκ = 0.99) and TIRI and P_ECO_2 (98% agreement, κ = 0.80, BCI 0.66, 0.89; pκ = 0.94) was high. The chance-corrected agreement between TIRI and the other 3 methods of airflow detection was better than agreements between Pn and thermistor or thermistor and P_ECO_2 (see Table 4).

DISCUSSION

To our knowledge, this study is the first of its kind to explore the accuracy and feasibility of noncontact sensing to detect airflow abnormalities during conventional polysomnography in a limited monitoring setting. We found a high degree of chance-corrected agreement between TIRI and conventional airflow sensors in subjects with and without a prior diagnosis of OSA. Patients with mild, moderate, and severe OSA were included in the study.

Because of a possible time delay in signal processing of data capture in the TIRI channel, we defined the scoring rules a priori, keeping in mind that "staggered events" in a conventional (Pn and thermistor) and TIRI channel could be secondary to recording delay. In fact, we did not find such a delay in these 3 channels, but events in CO_2 waveform were staggered due to the delayed response of the expired CO_2 to respiratory events, which were accounted for in our scoring rules.

The results of this study must be viewed with a certain degree of circumspection due to the short time of data collection and small sample size. This may not be considered a valid technology for use in sleep studies until it is evaluated thoroughly during full-night polysomnography. At the time of this study, we constrained ourselves to 1 to 2 hours of recording for practical reasons. TIRI produces massive data sets, and, before investing in an upgraded data-management infrastructure, we chose to evaluate this technology in a pilot study. Success on 1- to 2-hour recordings may not be considered as a complete clinical validation but justifies

Table 3—Breakdown of Concordant and Discordant Event Epochs Among Thermal Infrared Imaging, Nasal Pressure, Oronasal Thermistor and Expired CO_2

	Nasal Pressure		Oronasal thermistor		P_ECO_2	
	Event Epoch	Nonevent Epoch	Event Epoch	Nonevent Epoch	Event Epoch	Nonevent Epoch
TIRI						
Event Epoch	219	7	198	28	186	40
Nonevent Epoch	11	4208	7	4212	47	4172

TIRI refers to thermal infrared imaging; Pn, nasal pressure; P_ECO_2, expired carbon-dioxide.

future larger-scale efforts. Since the protocol did not require full-night polysomnography, subjects were studied early in the evening with consequently low sleep efficiency.

Nasal pressure has been validated in comparison to the gold standard, pneumotachometry, in assessing airflow during sleep and has been used effectively for scoring hypopneas and subtle airflow abnormalities such as respiratory effort-related arousals (RERAs).[21,22] At the current stage of development, TIRI is unable to detect respiratory events without apnea or oxygen desaturation such as RERAs in anyway comparable to Pn, and, hence, our study was limited to scoring of apneas and hypopneas. Thus, the results of pairwise comparison between TIRI and Pn are applicable only in the context of the definitions of hypopnea and apnea used in this study and cannot be extrapolated to include more subtle airflow abnormalities that Pn might detect. Our data also suggests that, when compared with Pn, TIRI appeared to perform better than thermistor in detecting these events (Table 4). In fact, with regard to the sensitivity of detecting respiratory events with apnea or hypopnea accompanied by a 4% oxygen desaturation when a combination of 3 channels were used as the reference standard, TIRI and Pn appeared to perform better than thermistor or P_ECO_2 (Table 2).

At the outset, both TIRI and thermistor measure temperature changes as a surrogate for airflow. Although it may be assumed that TIRI is only a substitute for thermistor, the results in Tables 2 and 4 could imply a more complex relationship. The chance-corrected agreement between thermistor and TIRI was excellent, as expected, but it was interesting to find that the agreement between Pn and TIRI was better than between Pn and thermistor (Table 4). To understand these results, one needs to bear in mind the following: TIRI passively acquires thermal information through natural radiation from the source. By contrast, the thermistor acquires thermal information through conduction while being embedded in the patient's oronasal airflow path. Conduction can be limited by heat absorption in the device, a time lag in the sensing of the thermal signal, and the properties of the metal in the thermistor. Thus, on theoretic grounds, the thermistor's measurement error has the potential of being larger than that of TIRI.

It is also important to understand that TIRI's close resemblance to thermistor is of meaning only because of the computational method used in this study that averages TIRI signal over the entire nasal measurement area to produce a single thermal value at every point in time. In other words, a 2-dimensional sensing modality is reduced to a single dimension, not unlike a "virtual thermistor." This simplifies mathematical modeling but abdicates a lot of useful information. However, this study was

Table 4—Chance-Corrected Agreements Estimated for Every Pairwise Combination of Airflow Channels Pairwise Comparison

	κ	95% BCI	Probability of κ being > 0.70
TIRI vs nasal pressure	0.83	0.70, 0.90	0.98
TIRI vs thermistor	0.92	0.86, 0.96	0.9998
TIRI vs P_ECO_2	0.80	0.66, 0.89	0.94
Nasal pressure vs thermistor	0.77	0.61, 0.78	0.87
Nasal pressure vs P_ECO_2	0.71	0.51, 0.84	0.61
Thermistor vs P_ECO_2	0.77	0.60, 0.87	0.84

TIRI refers to thermal infrared imaging; BCI, Bayesian credible interval; P_ECO_2, expired carbon-dioxide.

not designed to determine whether analysis of thermal information across the entire 2-dimensional nasal plane over time could enable TIRI to detect subtler phenomena such as RERAs and get closer to the performance of Pn.

To our knowledge, TIRI is the only method that would allow for retrospective analysis of collected data for detecting respiratory events. A clear view of the defined region of interest, e.g., oronasal area, at all times is the only requirement to process and analyze the data. This is achieved by the use of the tracking algorithm, which can compensate for minimal to moderate head motion. Changes in breathing pattern from nose to mouth can also be processed in real time or at a later time by redefining the region of interest. This powerful feature enables us to extract quality data from the recording, which might not be apparent in real time.

The TIRI system used in this study constitutes a unique prototype. The major cost in its implementation is the acquisition of a thermal camera. The price of an entry-level InSb Mid-Wave Infrared Camera from FLIR, Inc., is about $60,000 at this time. Due to the substantial size of the imagery data, sleep labs may need to upgrade their computing infrastructure, which will add to the initial cost. Being a noncontact sensor, TIRI can be completely unobtrusively during sleep and does not have the additional cost of sterilization or replacement of consumables, which minimizes the operating cost.

TIRI in its current form may be unable to reliably detect airflow abnormalities if the subject is breathing into an oronasal mask due to the distortion caused by the thermal signal as a result of dissipation of heat throughout the mask. This is the primary reason why pneumotachometry was not used as reference standard for airflow in our study.

Extreme situations, such as a subject covering his or her face with a thick blanket, could lead to complete loss of signal. However, in our study, we did not find a subject with a preference to sleep face down. This is in accord with a prior study of body position during nocturnal polysomnography,[8] which revealed very little prone sleep (0.6%) during such recordings, whereas prone sleep became more prevalent (8.4%) when the same subjects slept without polysomnographic monitoring. Thus, technical problems that may arise while monitoring the airflow signal in the prone position may not become clinically significant.

A new version of the software may enable real-time processing at a higher spatial resolution, from the current 320×256 up to 640×512 pixels. Increased spatial resolution will enable nuanced 2-dimensional computation of the breathing airflow, which may further enhance the characterization of hypopnea and more subtle airflow limitations not meeting the criteria for apnea or hypopnea.

In this feasibility study, we have demonstrated that TIRI, in a limited monitoring setting, is a practicable noncontact technology to detect apnea and hypopnea during polysomnography. Performance of TIRI during full-night polysomnography and its ability to detect nonapneic airflow-limitation events such as RERAs have to be extensively tested before recommending its use for routine clinical monitoring.

ACKNOWLEDGMENTS

DISCLOSURE STATEMENT

REFERENCES

1. Berry RB. Esophageal and Nasal Pressure Monitoring during Sleep. In: Lee-Chiong TL, Sateia M, Carskadon MA, eds. Sleep Medicine. Philadelphia, PA: Hanley & Belfus, Inc, 2002: 661-71.
2. Bornstein SK. Respiratory Monitoring During Sleep: Polysomnography. In: Guilleminault C, ed. Sleeping and Waking Disorders: Indications and Techniques. Stoneham, MA: Butterworth Publishers, 1982: 183-212.
3. Butkov N. Polysomnography. In: Lee-Chiong TL, Sateia M, Carskadon MA, eds. Sleep Medicine. Philadelphia, PA: Hanley & Belfus Inc, 2002: 605-37.
4. Cohn M. Respiratory Monitoring During Sleep: Respiratory Inductive Plethysmography. In: Guilleminault C, ed. Sleeping and Waking Disorders: Indications and Techniques. Stoneham, MA: Butterworth Publishers, 1982: 213-23.
5. Lee-Chiong TL. Monitoring Respiration during Sleep. In: Lee-Chiong TL, Sateia MJ, Carskadon MA, eds. Sleep Medicine. Philadelphia, PA: Hanley & Belfus, Inc, 2002: 639-46.
6. Edinger JD, Fins AI, Sullivan RJJ et al. Sleep in the laboratory and sleep at home: comparisons of older insomniacs and normal sleepers. Sleep 1997;20:1119-26.
7. Agnew HWJ, Webb WB, Williams RL. The first night effect: an EEG study of sleep. Psychophysiology 1966;2:263-66.
8. Metersky ML, Castriotta RJ. The effect of polysomnography on sleep position: possible implications on the diagnosis of positional obstructive sleep apnea. Respiration 1996;63:283-87.
9. Iber C, Ancoli-Israel S, Chesson A, Quan SF, eds. The AASM Manual for the Scoring of Sleep and Associated Events: Rules, Terminology and Technical Specifications. Westchester, IL: American Academy of Sleep Medicine, 2007.
10. The Report of an American Academy of Sleep Medicine Task Force. Sleep–Related Breathing Disorders in Adults: Recommendations for Syndrome Definition and Measurement Techniques in Clinical Research. SLEEP 1999;22:667.
11. Murthy R, Pavlidis I. Noncontact measurement of breathing function. Engineering in Medicine and Biology Magazine, IEEE 2006;25:57-67.
12. Fei J, Pavlidis I. Virtual thermistor. Conf Proc IEEE Eng Med Biol Soc 2007;2007:250-53.
13. Fei J, Pavlidis I. Thermistor at a Distance: Unobstrusive Measurement of Breath. IEEE Trans Biomed Eng. In press 2009.
14. Dowdall J, Pavlidis I, Tsiamyrtzis P. Coalitional Tracking. Computer Vision and Image Understanding 2007;106:205-19.
15. Murthy JN, Faiz S, Fei J, Abuelheiga A, Castriotta RJ. Remote Infra-Red Imaging: A Novel Non-Contact Method to Monitor Airflow During Polysomnography. Chest 2007;132:464a. (Abstract from Chest Meeting)
16. Murthy JN, vanJaarsveld J, Fei J, Pavlidis I, Harrykissoon RI, Castriotta RJ. Airflow Monitoring in Sleep Apnea Using Infra-Red Imaging. The American Journal of Respiratory and Critical Care Medicine 2008;A208.
17. Isard M, Blake A. Conditional density propagation for visual tracking. Int J Comp Vision 1998;29:5-28.
18. Heath M, Sarkar S, Sanocki T, Bowyer K. Comparison of Edge Detectors: A Methodology and Initial Study. Computer Vision and Pattern Recognition, IEEE Computer Society Conference on 1996;143.
19. Rechtschaffen A, Kales A, eds. A Manual of Standardized Terminology, Techniques and Scoring System for Sleep Stages of Human Subjects. Washington: 1968.
20. Castriotta RJ, Wilde MC, Lai JM, Atanasov S, Masel BE, Kuna ST. Prevalence and consequences of sleep disorders in traumatic brain injury. J Clin Sleep Med 2007;3:349-56.
21. Thurnheer R, Xie X, Bloch KE. Accuracy of nasal cannula pressure recordings for assessment of ventilation during sleep. Am J Respir Crit Care Med 2001;164:1914-19.
22. Heitman SJ, Atkar RS, Hajduk EA, Wanner RA, Flemons WW. Validation of nasal pressure for the identification of apneas/hypopneas during sleep. Am J Respir Crit Care Med 2002;166:386-91.

APPENDIX: STATISTICAL MODEL FOR K ESTIMATION

The usual approach to assessing agreement uses a set of independent and identically distributed trials (or epochs, in this case) in which each pair of devices generates a dichotomous signal indicating the presence or absence of an attribute (e.g., apnea, hypopnea). Obtaining a single pair of signals jointly from each device would have accomplished this over a large number of patients. The longitudinal approach adopted in this study, instead, uses a large number (119-181) of epochs from relatively few patients (14 controls and 13 patients with obstructive sleep apnea [OSA]). The primary statistical concern with the longitudinal approach is that the observed data comprises not one set of probabilities for the devices (a probability for each device and their joint probability), but a mixture of sets of probabilities so that the device probabilities and their joint probability varies from subject to subject. To properly address these issues, we adopt a Bayesian, longitudinal, random-effects, Bernoulli model that accounts for the device (thermal infrared imaging [TIRI], nasal pressure [Pn], oronasal thermistor, or end carbon-dioxide [P_ECO_2]) probabilities, their corresponding joint probability, and each subject's influence on these probabilities.

We use a model in which the probability of a device's dichotomous response is a function of a subject effect and a device effect but is otherwise independent across epochs. For each pair of devices, we also construct an "agreement sequence" depicting the joint agreement between the 2 devices across epochs. For each of these agreement sequences, we likewise assume that the dichotomous agreement response is a function of the same subject and an effect representing the joint tendency for the devices to agree but are otherwise independent across epochs. We also assume that, for a given subject, device responses are independent between devices, as are the agreement responses between any pair of devices.

The subject effect was assumed to be random, following a normal distribution, and the device effects and agreement effects were assumed to be fixed. To complete the Bayesian specification, vague or weakly informative prior distributions were adopted for the parameters. Markov chain Monte Carlo methods were used to obtain the posterior distributions. The posterior distributions of the probability of a response for device averaging over subject effects, the posterior probability of agreement for device pair averaging over subject effects, and the posterior probability of the coefficient of agreement were obtained. The Markov chain Monte Carlo analysis was conducted in Open-BUGS 3.0.3, and additional analyses were conducted in R 2.6.2 and STATA 10.